Particle flow superpositional GLMB filter

Augustin-Alexandru Saucan[a], Yunpeng Li[a], and Mark Coates[a]

[a] Department of Electrical & Computer Engineering, McGill University,
3480 University Street, Montreal, Quebec, Canada

ABSTRACT

In this paper we propose a Superpositional Marginalized δ-GLMB (SMδ-GLMB) filter for multi-target tracking and we provide bootstrap and particle flow particle filter implementations. Particle filter implementations of the marginalized δ-GLMB filter are computationally demanding. As a first contribution we show that for the specific case of superpositional observation models, a reduced complexity update step can be achieved by employing a superpositional change of variables. The resulting SMδ-GLMB filter can be readily implemented using the unscented Kalman filter or particle filtering methods.

As a second contribution, we employ particle flow to produce a measurement-driven importance distribution that serves as a proposal in the SMδ-GLMB particle filter. In high-dimensional state systems or for highly-informative observations the generic particle filter often suffers from weight degeneracy or otherwise requires a prohibitively large number of particles. Particle flow avoids particle weight degeneracy by guiding particles to regions where the posterior is significant. Numerical simulations showcase the reduced complexity and improved performance of the bootstrap SMδ-GLMB filter with respect to the bootstrap Mδ-GLMB filter. The particle flow SMδ-GLMB filter further improves the accuracy of track estimates for highly informative measurements.

Keywords: random finite sets, δ-GLMB filter, particle filter, particle flow, track before detect, superpositional model.

1. INTRODUCTION

In general, radar and sonar systems are employed to detect, localize and track various targets. Target tracking systems can be classified into Track While Scan (TWS) and Track Before Detect (TBD) systems. In TWS systems the sensor signals are pre-processed in order to obtain a set of point-measurements that contain a noisy measurement for each detected target and clutter points, i.e., false alarms. The associations between targets and measurements are unknown and the resulting incertitude is referred to as origin uncertainty. Probabilistic data association[1–3] filters have been developed to associate the detected points with tracks and eliminate clutter. Alternatively, the Probability Hypothesis Density (PHD) filter[4] models the set of multiple targets as a Random Finite Set (RFS) and propagates the first-order moment (called PHD or intensity function) of the RFS posterior. The PHD filter avoids the explicit association step of classical probabilistic data association filters.[1] Within the TWS framework, the PHD filter has found numerous applications in diverse fields.[5–8] More recently, the δ-Generalized Labeled Multi-Bernoulli (δ-GLMB) RFS density[9] was proposed as a conjugate prior for point-measurement model and tractable filters were proposed by Vo et al.[10,11]

Filters developed within the TBD framework track targets directly from the sensor signals, without the need for pre-processing (detection and estimation) procedures. For the specific case of a separable likelihood function, a TBD-Multi-Bernoulli filter has been proposed.[12] However, in practice the separable likelihood model is only a valid approximation if the targets are sufficiently separated. Additionally, the separable likelihood condition is not achieved by several important types of superpositional sensors, e.g., those that record the sum of individual target-generated (or backscattered) signals. Accordingly, superpositional PHD and CPHD filters were proposed for acoustical amplitude sensors and radio-frequency tomography[13] and for phased-arrays.[14] Contrary to the TWS case, the δ-GLMB density no longer represents a conjugate prior for the likelihood function induced by the superpositional observation model. For superpositional amplitude models, Papi et al. have developed a

Further author information: (Send correspondence to A. Saucan)
A. Saucan: E-mail: augustin.saucan@mail.mcgill.ca, Telephone: 1 514 398 5516

particle implementation of the GLMB filter.[15] This filter employs the superpositional CPHD filter to construct a proposal density. For a generic observation model, including the superpositional case, Papi et al. propose a marginalized δ-GLMB (Mδ-GLMB) that approximates the true posterior with a δ-GLMB density that minimizes the Kullback-Leibler divergence from the true posterior.[16]

In this paper, we focus on superpositional observation models and develop a tractable alternative to the Mδ-GLMB filter. We describe two particle filter implementations. A direct particle implementation of the Mδ-GLMB filter is computationally intensive due to the Cartesian product of target particle sets required in the marginalization step. In order to avoid this step, we propose the Superpositional Mδ-GLMB (SMδ-GLMB) filter that relies on a change of variables similar to the superpositional PHD filter[13] followed by a Gaussian approximation. We provide a Bootstrap Particle Filter[17] implementation of the SMδ-GLMB (BPF-SMδ-GLMB) filter. Additionally, we extend the previous implementation by using particle flow as a means to produce measurement-driven importance distributions. The resulting implementation is referred to as the Particle Flow Particle Filter SMδ-GLMB (PFPF-SMδ-GLMB) filter. Particle flow particle filters[18] where shown to offer superior performance with respect to the standard bootstrap particle filter for high-dimensional state systems or highly-informative measurements. The particle flow proposal takes into account the current measurement and is capable of generating samples in regions where the posterior is significant and hence avoids particle weight degeneracy. In this work we rely on the particle filter particle flow developed by Li et al.[18] for which the flow proposal and the prior distributions are linked through a bijective transformation, allowing the importance weights to be easily computed.

The article is structured as follows. A brief overview of labeled multi-target tracking along with the main challenge of the particle Mδ-GLMB filter is presented in Section 2. The SMδ-GLMB filter is derived in Section 3. We also describe the bootstrap and particle flow implementations in this section. In Section 4 we present the results of our numerical experiments and we conclude in Section 5.

2. BACKGROUND AND PROBLEM FORMULATION

In order to incorporate target tracks into the Bayes multi-target filtering framework, targets are identified by a label. The state of a labeled target, denoted with $\mathbf{x} = (x, l)$, is comprised of the target state $x \in \mathbb{X}$ and label $l \in \mathbb{L}$. The multi-target state $\boldsymbol{X}_k = \{\boldsymbol{x}_{k,1}, \cdots, \boldsymbol{x}_{k,N(k)}\}$ is modeled as a Random Finite Set (RFS),[19] where the number of targets as well as the individual target states are random.

In TBD systems, the set of multiple targets $\boldsymbol{X}_k$ is observed via the measurement vector $z_k \in \mathbb{Z}$. The objective is the estimation of the labeled multi-target posterior density $\boldsymbol{\pi}_k(\boldsymbol{X}_k|z_{0:k})$, which captures all information of the target states and labels given the measurement history $z_{0:k} = \{z_0, \ldots, z_k\}$. The multi-target Bayes filter[4] propagates $\boldsymbol{\pi}_k$ in time according to

$$\boldsymbol{\pi}_k(\boldsymbol{X}_k|z_{0:k}) = \frac{\boldsymbol{h}(z_k|\boldsymbol{X}_k)\boldsymbol{\pi}_{k|k-1}(\boldsymbol{X}_k)}{\int \boldsymbol{h}(z_k|\boldsymbol{X})\boldsymbol{\pi}_{k|k-1}(\boldsymbol{X})\delta\boldsymbol{X}} \tag{1}$$

$$\boldsymbol{\pi}_{k+1|k}(\boldsymbol{X}_{k+1}) = \int \boldsymbol{f}_{k+1|k}(\boldsymbol{X}_{k+1}|\boldsymbol{X}_k)\boldsymbol{\pi}_k(\boldsymbol{X}_k|z_{0:k})\delta\boldsymbol{X}_k, \tag{2}$$

where $\boldsymbol{f}_{k+1|k}(\boldsymbol{X}_{k+1}|\boldsymbol{X}_k)$ is the RFS counterpart of the single target transition kernel $f_{k+1|k}(x_{k+1}|x_k, l)$. Additionally, the likelihood $\boldsymbol{h}(z_k|\boldsymbol{X}_k)$ is induced by the superpositional observation model

$$z_k = \sum_{(x,l)\in\boldsymbol{X}_k} g_k(x, l) + w_k, \tag{3}$$

where $w_k \sim \mathcal{N}(0, R_k)$ is the measurement noise assumed a Gaussian and independent of the targets. Note that the sensor observation z_k is given by the superposition of the individual target contributions $g_k(x, l)$, which in radar/sonar systems would represent the signal backscattered or generated by the respective targets.

The set integral in the case of labeled RFSes is defined[19] as

$$\int f(\boldsymbol{X})\delta\boldsymbol{X} \triangleq \sum_{n=0}^{\infty} \frac{1}{n!} \sum_{(l_1,\ldots,l_n)\in\mathbb{L}^n} \int_{\mathbb{X}^n} f(\{(x_1, l_1), \ldots, (x_n, l_n)\})\, dx_1 \cdots dx_n, \tag{4}$$

for a function $f : \mathcal{F}(\mathbb{X} \times \mathbb{L}) \to \mathbb{R}$ and where $\mathcal{F}(\mathbb{X} \times \mathbb{L})$ represents the collection of all finite labeled RFS with elements in $\mathbb{X} \times \mathbb{L}$.

Throughout the paper, we use the standard inner product notation $\langle f, g \rangle \triangleq \int_{\mathbb{X}} f(x)g(x)dx$ and the following multi-object exponential

$$h^{\boldsymbol{X}} \triangleq \prod_{\boldsymbol{x} \in \boldsymbol{X}} h(\boldsymbol{x}), \tag{5}$$

where $h : \mathbb{X} \times \mathbb{L} \to \mathbb{R}$ and by convention $h^{\emptyset} = 1$. A generalized Kronecker delta is defined for various types of arguments (e.g, integers, vectors, sets) as

$$\delta_{\boldsymbol{Y}}(\boldsymbol{X}) = \begin{cases} 1, & \text{if } \boldsymbol{X} = \boldsymbol{Y} \\ 0, & \text{otherwise.} \end{cases} \tag{6}$$

A set indicator function is introduced as

$$1_{\boldsymbol{Y}}(\boldsymbol{X}) = \begin{cases} 1, & \text{if } \boldsymbol{X} \subseteq \boldsymbol{Y} \\ 0, & \text{otherwise.} \end{cases} \tag{7}$$

Note that we employ $1_{\boldsymbol{Y}}(\boldsymbol{x})$ in place of $1_{\boldsymbol{Y}}(\{\boldsymbol{x}\})$.

In the following we briefly review the family of δ-GLMB densities and we introduce the Mδ-GLMB filter. Subsequently, we present the limitations of a straightforward particle-filter implementation of the Mδ-GLMB filter.

2.1 The Mδ-GLMB filter

The δ-GLMB family of multi-target densities[9,10] permits the development of a closed form solution to the Chapman-Kolmogorov (2) and the Bayes multi-target update equation for the point-measurement model. To ensure distinct labels we employ the pair (k, i) as a label for a target born at time k, where i is a unique index required to distinguish targets born at the same time.[9,10] The label space for a target born at time k is denoted $\mathbb{L}_k$ while the label space of a target at time k (including those born prior to time k) is denoted $\mathbb{L}_{0:k}$. Note that $\mathbb{L}_{0:k} = \mathbb{L}_{0:k-1} \cup \mathbb{L}_k$ and that $\mathbb{L}_k \cap \mathbb{L}_{0:k-1} = \emptyset$.

A multi-target labeled set $\boldsymbol{X}_k$ is an element of $\mathcal{F}(\mathbb{X} \times \mathbb{L}_{0:k})$, i.e., the set of all finite sets with elements from $\mathbb{X} \times \mathbb{L}_{0:k}$. A δ-GLMB density for the RFS $\boldsymbol{X}_k$ can be expressed as

$$\boldsymbol{\pi}_k(\boldsymbol{X}) = \Delta(\boldsymbol{X}) \sum_{I \in \mathcal{F}(\mathbb{L}_{0:k})} \delta_I(\mathcal{L}(\boldsymbol{X})) w_k^{(I)} \left[p_k^{(I)}\right]^{\boldsymbol{X}}, \tag{8}$$

where we define the label projection $\mathcal{L}(\{(x_1, l_1), \ldots, (x_n, l_n)\}) = \{l_1, \ldots, l_n\}$ and $\Delta(\boldsymbol{X})$ is the distinct label indicator defined as

$$\Delta(\boldsymbol{X}) \triangleq \begin{cases} 1, & \text{if } |\mathcal{L}(\boldsymbol{X})| = |\boldsymbol{X}| \\ 0, & \text{otherwise.} \end{cases}$$

The summation terms in (8) are usually referred to as hypotheses and correspond to all finite label sets $I \in \mathcal{F}(\mathbb{L}_{0:k})$. Note that for a given hypothesis I, $p_k^{(I)}(\cdot, l)$ is a density on $\mathbb{X}$ and the weights $w_k^{(I)}$ are non-negative with $\sum_{I \in \mathcal{F}(\mathbb{L}_{0:k})} w_k^{(I)} = 1$. The propagation of the δ-GLMB density is achieved through prediction and update. For the point measurement model, both Gaussian mixture and SMC implementations were developed by Vo et al.[10] and in the following sections we give a brief overview of the prediction and update steps for the superpositional model of (1).

2.1.1 Mδ-GLMB prediction

The measurement z_k is not involved in the prediction of (2) and hence the prediction stage of the Mδ-GLMB filter is similar to the prediction of the δ-GLMB filter.[9] In order to account for target births at time k, we introduce the labeled multi-target set $\boldsymbol{Y}$ with density $\boldsymbol{f}_B(\boldsymbol{Y})$ defined as

$$\boldsymbol{f}_B(\boldsymbol{Y}) = \Delta(\boldsymbol{Y}) w_B(\mathcal{L}(\boldsymbol{Y})) \left[p_B\right]^{\boldsymbol{Y}}, \tag{9}$$

where $w_B(\mathcal{L}(\boldsymbol{Y}))$ is the weight of the set of birth targets $\boldsymbol{Y}$ and $p_B(x,l)$ with $l \in \mathcal{L}(\boldsymbol{Y})$ are their probability densities. The birth density of (9) includes the labeled Poisson, labeled iid and labeled multi-Bernoulli densities.[9]

Following,[9] if the current multi-target filtering density is a δ-GLMB of the form (8), then the predicted density is also a δ-GLMB given by

$$\boldsymbol{\pi}_{k+1|k}(\boldsymbol{X}) = \Delta(\boldsymbol{X}) \sum_{I \in \mathcal{F}(\mathbb{L}_{0:k+1})} \delta_I(\mathcal{L}(\boldsymbol{X})) w_{k+1|k}^{(I)} \left[p_{k+1|k}^{(I)}\right]^{\boldsymbol{X}}, \tag{10}$$

where

$$\begin{aligned}
w_{k+1|k}^{(I)} &= w_S^{(I)}(I \cap \mathbb{L}_{0:k}) w_B(I \cap \mathbb{L}_{k+1}), \\
w_S^{(I)}(L) &= \left[\eta_S^{(I)}\right]^L \sum_{J \subseteq \mathbb{L}_{0:k}} 1_J(L) \left[1 - \eta_S^{(I)}\right]^{J \setminus L} w_k^{(J)}, \\
\eta_S^{(I)}(l) &= \langle p_S(\cdot, l), p_k^{(I)}(\cdot, l) \rangle, \\
p_{k+1|k}^{(I)}(x,l) &= 1_{\mathbb{L}_{0:k}}(l) p_S^{(I)}(x,l) + 1_{\mathbb{L}_{k+1}}(l) p_B(x,l) \\
p_S^{(I)}(x,l) &= \frac{1}{\eta_S^{(I)}(l)} \langle p_S(\cdot, l) f_{k+1|k}(x|\cdot, l), p_k^{(I)}(\cdot, l) \rangle,
\end{aligned}$$

and where $f_{k+1|k}(x|\cdot, l)$ is the single target kinematic transition kernel and $p_S(\cdot, l)$ is the probability of survival. The birth parameters $p_B(\cdot, l)$ and $w_B(L)$ are given by the birth density of (9).

2.1.2 Mδ-GLMB update

The update stage of the Mδ-GLMB filter employs the current measurement vector z_{k+1} to correct the predicted $\boldsymbol{\pi}_{k+1|k}(\cdot)$ δ-GLMB density and approximates the resulting RFS posterior with a δ-GLMB density of the form

$$\boldsymbol{\pi}_{k+1}(\boldsymbol{X}) \approx \Delta(\boldsymbol{X}) \sum_{I \in \mathcal{F}(\mathbb{L}_{0:k+1})} w_{k+1}^{(I)} \delta_I(\mathcal{L}(\boldsymbol{X})) \left[\hat{p}_{k+1}^{(I)}\right]^{\boldsymbol{X}}, \tag{11}$$

where for a label set $I = \{l_1, \ldots, l_n\}$ the following relationships hold:

$$w_{k+1}^{(I)} \propto w_{k+1|k}^{(I)} \eta_{z_{k+1}}(I), \tag{12}$$

$$\eta_{z_{k+1}}(I) = \int \cdots \int_{\mathbb{X}^n} h_{k+1}(z_{k+1}|(x_1,l_1), \ldots, (x_n,l_n)) \prod_{j=1}^{n} \left[p_{k+1|k}^{(I)}(x_j, l_j)\right] dx_1 \cdots dx_n, \tag{13}$$

$$\hat{p}_{k+1}^{(I)}(x_i, l_i) = \frac{1_I(l_i)}{\eta_{z_{k+1}}(I)} p_{k+1|k}^{(I)}(x_i, l_i) \tilde{h}_{\bar{i}}(z_{k+1}|x_i, l_i), \quad \forall \ i = 1, \ldots, n, \tag{14}$$

$$\tilde{h}_{\bar{i}}(z_{k+1}|x_i, l_i) = \int \cdots \int_{\mathbb{X}^{n-1}} h_{k+1}(z_{k+1}|(x_1,l_1), \ldots, (x_n,l_n)) \prod_{\substack{j=1 \\ j \neq i}}^{n} \left[p_{k+1|k}^{(I)}(x_j, l_j)\right] dx_1 \cdots dx_{i-1} dx_{i+1} \cdots dx_n. \tag{15}$$

The modified likelihood of $\tilde{h}_{\bar{i}}(z_{k+1}|x_i, l_i)$ of (15) is obtained by marginalizing the exact likelihood over all target densities in the set $I \setminus \{i\}$ (i.e., all targets in I except for the target for which the update is being performed).

The joint posterior of the target set is approximated as the product of marginalized posteriors $\left[\hat{p}_{k+1}^{(I)}\right]^{\boldsymbol{X}}$. The Bayes normalization constant $\eta_{z_{k+1}}(I)$ of (13) effectively represents the evidence that this specific set of targets I explains the measurement z_{k+1}. The updated hypothesis weight $w_{k+1}^{(I)}$ is exact, and the marginalization process only involves the target densities of a specific hypothesis. Papi et al. show that the approximations of (12), (13), and (14) lead to an approximate δ-GLMB density that minimizes the Kullback-Leibler divergence from the exact posterior $\boldsymbol{\pi}_k(\cdot)$ and matches its PHD function and cardinality distribution.[16] Particle filter implementations of the Mδ-GLMB filter are usually employed since the observation likelihood $h_k(\cdot|\boldsymbol{X}_k)$ is non-linear. In the following, we highlight the computational challenges associated with such particle filter implementations.

2.2 The computational challenge for sequential Monte Carlo implementations

For a sequential Monte Carlo (SMC) approximation of the Mδ-GLMB filter, we consider that each predicted single target density $p_{k+1|k}^{(I)}(\cdot,l)$ is approximated with a set of weighted particles $\{(\omega_{k+1|k}^{j}(l), x_{k+1|k}^{j}(l))\}_{j=1}^{N}$. Then, equations (13) and (14) become

$$\eta_{z_{k+1}}(I) \approx \sum_{j_1=1}^{N} \cdots \sum_{j_n=1}^{N} h_{k+1}(z_{k+1}|(x_{k+1|k}^{j_1}(l_1), l_1), \ldots, (x_{k+1|k}^{j_n}(l_n), l_n))\omega_{k+1|k}^{j_1}(l_1)\cdots\omega_{k+1|k}^{j_n}(l_n), \tag{16}$$

$$\hat{p}_{k+1}^{(I)}(x_i, l_i) \approx \frac{1_I(l_i)}{\eta_{z_{k+1}}(I)} \sum_{j_1=1}^{N} \omega_{k+1|k}^{j_i}(l_i)\tilde{h}_{\bar{i}}(z_{k+1}|x_{k+1|k}^{j_i}(l_i), l_i)\delta_{x_{k+1|k}^{j_i}(l_i)}(x_i) \tag{17}$$

$$\begin{aligned}\tilde{h}_{\bar{i}}(z_{k+1}|x_{k+1|k}^{j_i}(l_i), l_i) \approx \sum_{j_1=1}^{N} \cdots \sum_{j_{i-1}=1}^{N} \sum_{j_{i+1}=1}^{N} \cdots \sum_{j_n=1}^{N} & h_{k+1}(z_{k+1}|(x_{k+1|k}^{j_1}(l_1), l_1), \ldots, (x_{k+1|k}^{j_n}(l_n), l_n)) \\ & \times \omega_{k+1|k}^{j_1}(l_1)\cdots\omega_{k+1|k}^{j_{i-1}}(l_{i-1})\omega_{k+1|k}^{j_{i+1}}(l_{i+1})\cdots\omega_{k+1|k}^{j_n}(l_n).\end{aligned} \tag{18}$$

Notice that the above summations involve the mixing, i.e., the n-fold Cartesian product, of the particle sets in the current label set I. Except for the scenario where the number of targets n is very small, the computational complexity of this operation is prohibitively large. Computing (16) involves N^n additions. In the following section, we provide computationally tractable particle filter approximations that avoid the n-fold Cartesian product of the target particle sets.

3. COMPUTATIONALLY TRACTABLE SMC Mδ-GLMB FILTERS

In this section we present approximate tractable SMC implementations of the Mδ-GLMB filter. First, we propose a Truncated Bootstrap Particle Filter Mδ-GLMB (TBPF Mδ-GLMB) filter that employs a reduced number $M \ll N^n$ of n-tuples in order order to approximate (16) and (18). Second, we develop the BPF Superpositional Mδ-GLMB (BPF-SMδ-GLMB) filter which relies on a change of variables and a Gaussian approximation in order to avoid the Cartesian product of particle sets. Third, we propose a Particle Flow Particle Filter PFPF-SMδ-GLMB implementation that uses particle flow to guide particles into regions where the posterior is significant and hence improves the precision of track estimates.

3.1 The truncated BPFδ-GLMB filter

The TBPFδ-GLMB filter achieves a reduced complexity implementation of (16) and (18) by using only a selected number of particle n-tuples as opposed to using all N^n n-tuples. We consider that each predicted single target density $p_{k+1|k}^{(I)}(\cdot,l)$ is approximated with a set of weighted particles $\{(\omega_{k+1|k}^{j}(l), x_{k+1|k}^{j}(l))\}_{j=1}^{N}$. Next we consider a set of particle indices $\Upsilon = \{\upsilon = (\upsilon_1, \ldots, \upsilon_n)|\upsilon_1 \in [1, N], \ldots, \upsilon_n \in [1, N]\}$ where the cardinality of $|\Upsilon| \ll N^n$. The set Υ can be obtained by uniformly sampling n-tuples without replacement from the space $[1, N]\times\cdots\times[1, N]$ obtained as the n-fold product of the integer sets $[1, N]$. The set of n-tuples Υ can be employed to obtain a reduced complexity estimate of the model evidence term $\eta_{z_{k+1}}(I)$ of (16).

Direct evaluation of the modified likelihood of (18) requires the computation of likelihoods and weight products associated with $N^{(n-1)}$ $(n-1)$-tuples. However, using a set $\Upsilon_i = \{\upsilon = (\upsilon_1, \ldots, \upsilon_{i-1}, \upsilon_{i+1}, \ldots, \upsilon_n) | \upsilon_k \in [1,\, N], k = 1, \ldots, i-1, i+1, \ldots, n\}$ of unique $(n-1)$-tuples, $\tilde{h}_{\bar{i}}(\cdot)$ (18) can be approximated as

$$\begin{aligned}\tilde{h}_{\bar{i}}(z_{k+1}|x_i, l_i) \approx \sum_{\upsilon \in \Upsilon_i} & h_{k+1}(z_{k+1}|(x^{\upsilon_1}_{k+1|k}(l_1), l_1), \ldots, (x_i, l_i) \cdots, (x^{\upsilon_n}_{k+1|k}(l_n), l_n)) \\ & \times \bar{\omega}^{\upsilon_1}_{k+1|k}(l_1) \cdots \bar{\omega}^{\upsilon_{i-1}}_{k+1|k}(l_{i-1}) \bar{\omega}^{\upsilon_{i+1}}_{k+1|k}(l_{i+1}) \cdots \bar{\omega}^{\upsilon_n}_{k+1|k}(l_n),\end{aligned} \tag{19}$$

where the weights of the $(n-1)$-tuples given by Υ_i must be normalized, i.e.,

$$\sum_{\upsilon \in \Upsilon_i} \bar{\omega}^{\upsilon_1}_{k+1|k}(l_1) \cdots \bar{\omega}^{\upsilon_{i-1}}_{k+1|k}(l_{i-1}) \bar{\omega}^{\upsilon_{i+1}}_{k+1|k}(l_{i+1}) \cdots \bar{\omega}^{\upsilon_n}_{k+1|k}(l_n) = 1,$$

in order to represent a particle approximation of the joint density of the target set $I \setminus l_i$.

By evaluating $\tilde{h}_{\bar{i}}(z_{k+1}|x_i, l_i)$ for each particle of the i-th target, the updated posterior is obtained via (17) and involves a total of $N \cdot |\Upsilon_i|$ additions. The model evidence term $\eta_{z_{k+1}}(I)$ of (16) can also be approximated as the Bayes normalization constant resulting from the updated posterior of (17).

3.2 The SMδ-GLMB filter

By employing the specific superpositional observation model of (3) and assuming the observation noise is Gaussian, $w_k \sim \mathcal{N}(0, R_k)$, we can rewrite (13) as

$$\eta_{z_{k+1}}(I) = \int \cdots \int_{\mathbb{X}^n} \mathcal{N}(z_{k+1}; \sum_{i=1}^{n} g_{k+1}(x_i, l_i), R_{k+1}) \prod_{j=1}^{n} \left[p^{(I)}_{k+1|k}(x_j, l_j) \right] dx_1 \cdots dx_n, \tag{20}$$

where $\mathcal{N}(z; \mu, \Sigma)$ stands for the Gaussian density function evaluated at z with mean μ and covariance Σ. Furthermore, if we employ the change of variables $y = \sum_{i=1}^{n} g_{k+1}(x_i, l_i)$, we can rewrite (20) using a single integral as

$$\eta_{z_{k+1}}(I) = \int_{\mathbb{Z}} \mathcal{N}(z_{k+1}; y, R_{k+1}) p(y) dy\,. \tag{21}$$

By assuming $p(y) \approx \mathcal{N}(\mu, \Sigma)$, the integral reduces to

$$\eta_{z_{k+1}}(I) \approx \mathcal{N}(z_{k+1}; \mu, R_{k+1} + \Sigma). \tag{22}$$

The Gaussian assumption on the distribution of y is equivalent to assuming that

$$\sum_{i=1}^{n} g_{k+1}(x_i, l_i) \Big| \mathcal{L}(\boldsymbol{X}_{k+1}) = \{l_1, \ldots, l_n\} \sim \mathcal{N}(\mu, \Sigma), \tag{23}$$

where the parameters of the Gaussian distribution are approximately given by

$$\begin{aligned}\mu_i &\triangleq \sum_{j=1}^{N} \omega^{j}_{k+1|k}(l_i) g_{k+1}(x^{j}_{k+1|k}(l_i)) \\ \mu &\approx \sum_{i=1}^{n} \mu_i, \qquad (24) \\ \Sigma &\approx \sum_{i=1}^{n} \left[\sum_{j_i=1}^{N} \omega^{j_i}_{k+1|k}(l_i) g_{k+1}(x^{j_i}_{k+1|k}(l_i)) \left[g_{k+1}(x^{j_i}_{k+1|k}(l_i)) \right]^T - \mu_i \mu_i^T \right]. \qquad (25)\end{aligned}$$

The case of $\tilde{h}_{\bar{i}}(z_{k+1}|x_i, l_i)$ follows along similar lines:

$$\begin{aligned}\tilde{h}_{\bar{i}}(z_{k+1}|x_i, l_i) &= \int \cdots \int_{\mathbb{X}^{n-1}} \mathcal{N}(z_{k+1}; \sum_{j=1}^{n} g_{k+1}(x_j, l_j), R_{k+1}) \\ &\qquad \times \prod_{\substack{j=1 \\ j\neq i}}^{n} \left[p^{(I)}_{k+1|k}(x_j, l_j)\right] dx_1 \cdots dx_{i-1} dx_{i+1} \cdots dx_n \\ &= \int_{\mathbb{Z}} \mathcal{N}(z_{k+1}; g_{k+1}(x_i, l_i) + y_{\bar{i}},\, R_{k+1}) p(y_{\bar{i}}) dy_{\bar{i}}, \\ &\approx \mathcal{N}\left(z_{k+1}; g_{k+1}(x_i, l_i) + \mu_{\bar{i}},\, R_{k+1} + \Sigma_{\bar{i}}\right), \end{aligned} \tag{26}$$

where in the second equation we employed the change of variables $y_{\bar{i}} = \sum_{j=1,\, j\neq i}^{n} g_{k+1}(x_j, l_j)$ while to obtain the final result we assumed $p(y_{\bar{i}}) = \mathcal{N}(\mu_{\bar{i}}, \Sigma_{\bar{i}})$. The parameters of the Gaussian distribution can be obtained approximately as

$$\mu_{\bar{i}} \approx \mu - \sum_{j_i=1}^{N} \omega^{j_i}_{k+1|k}(l_i) g_{k+1}(x^{j_i}_{k+1|k}(l_i)), \tag{27}$$

$$\Sigma_{\bar{i}} \approx \Sigma - \sum_{j_i=1}^{N} \omega^{j_i}_{k+1|k}(l_i) g_{k+1}(x^{j_i}_{k+1|k}(l_i)) \left[g_{k+1}(x^{j_i}_{k+1|k}(l_i))\right]^T + \mu_i \mu_i^T. \tag{28}$$

Finally, from (26) and (14) the posterior $\hat{p}^{(I)}_{k+1}(x_i, l_i)$ is

$$\hat{p}^{(I)}_{k+1}(x_i, l_i) \approx 1_I(l_i) \frac{p^{(I)}_{k+1|k}(x_i, l_i)\, \mathcal{N}\left(z_{k+1}; g_{k+1}(x_i, l_i) + \mu_{\bar{i}},\, R_{k+1} + \Sigma_{\bar{i}}\right)}{\int_{\mathbb{X}} p^{(I)}_{k+1|k}(x_i, l_i)\, \mathcal{N}\left(z_{k+1}; g_{k+1}(x_i, l_i) + \mu_{\bar{i}},\, R_{k+1} + \Sigma_{\bar{i}}\right) dx}. \tag{29}$$

When the particles $\{(\omega^{j_i}_{k+1|k}(l_i), x^{j_i}_{k+1|k}(l_i))\}_{j_i=1}^{N}$ for $i = 1, \ldots n$ are propagated using only the kinematic kernel, the above equations lead to the Bootstrap Particle Filter SMδ-GLMB (BPF-SMδ-GLMB) filter. In this case, the posterior (29) for target l_i becomes

$$\hat{p}^{(I)}_{k+1}(x_i, l_i) \approx \frac{1_I(l_i)}{K} \sum_{j_i=1}^{N} \omega^{j_i}_{k+1|k}(l_i)\, \tilde{h}_{\bar{i}}(z_{k+1}|x^{j_i}_{k+1|k}(l_i), l_i) \delta_{x^{j_i}_{k+1|k}(l_i)}(x_i) \qquad \forall\, i = 1, \ldots, n, \tag{30}$$

where K is a normalization constant. Additionally, an Unscented Kalman Filter (UKF)[20,21] implementation is also possible, leading to a UKF-SMδ-GLMB filter.

3.3 The PFPF-SMδ-GLMB filter

In this section we propose a particle flow particle filter SMδ-GLMB (PFPF-SMδ-GLMB) filter. Proceeding in a similar manner to,[22] we separate legacy and birth targets and compute accordingly their particle flow.

At time step k and for each legacy target with label $l_i \in I$ and particle set $\{(\omega^{j_i}_k(l_i), x^{j_i}_k(l_i))\}_{j_i=1}^{N}$, the particle flow particle filter (PF-PF)[18] first propagates the j_i-th particle using the kinematic model: $\eta^{j_i}_0 \sim f_{k+1|k}(\cdot|x^{j_i}_k(l_i), l_i)$. Second, using the modified likelihood of (26), we construct an invertible mapping $\eta^{j_i}_1 = T^{j_i}(\eta^{j_i}_0)$ that transports $\eta^{j_i}_0$ via particle flow into regions where the posterior density of (29) is significant. The transformation is a continuous transport indexed by the pseudo-time $\lambda \in [0, 1]$.

The mapping is defined by an Ordinary Differential Equation (ODE) (see Li and Coates[18] for details). In practice a finite series of transformations is applied to approximate the discretized integration of the ODE with initial value η^i_0. For Gaussian systems with non-linear measurement equations, two numerical solutions exist for

$\zeta(\eta_\lambda^i, \lambda)$. The exact Daum and Huang (EDH)[23] filter is computationally simpler; the localized Daum and Huang (LEDH)[24] filter can be more accurate in some settings.

Li and Coates prove that under mild assumptions on the smoothness of the measurement function, an invertible mapping is achievable between $\eta_1^{j_i}$ and $\eta_0^{j_i}$ and the importance distribution becomes:[18]

$$q(\eta_1^{j_i}|x_k^{j_i}, l_i, z_{k+1}) = \frac{p(\eta_0^{j_i}|x_k^{j_i})}{|\det(\dot{T}^{j_i}(\eta_0^{j_i}))|}, \tag{31}$$

where $p(\eta_0^{j_i}|x_k^{j_i})$ is a prior distribution and $|\det(\dot{T}^{j_i}(\eta_0^{j_i}))|$ represents the absolute value of the Jacobian determinant of the mapping $T^{j_i}(\cdot)$. In the EDH version of the PF-PF, the evaluation of the determinant is avoided since the same mapping is applied to all particles while in the LEDH version of the PF-PF, the evaluation is straightforward since the mapping is a series of affine transformations. Li and Coates provide implementation details for both EDH and LEDH variants of the particle flow particle filter.[18]

According to (30), the updated density $\hat{p}_{k+1}^{(I)}(x_i, l_i)$ is approximated by the particle set $\{(\omega_{k+1}^{j_i}, \eta_1^{j_i})\}_{j_i=1}^N$ with weights

$$\omega_{k+1}^{j_i} \propto \frac{\tilde{h}_{\bar{i}}(z_{k+1}|\eta_1^{j_i}, l_i) f_{k+1|k}(\eta_1^{j_i}|x_k^{j_i}, l_i) p_S(x_k^{j_i}, l_i)}{q(\eta_1^{j_i}|x_k^{j_i}, l_i, z_{k+1})} \omega_k^{j_i}. \tag{32}$$

Furthermore, by employing the mapping property of the invertible flow (31), the weights become

$$\omega_{k+1}^{j_i} \propto \frac{\tilde{h}_{\bar{i}}(z_{k+1}|\eta_1^{j_i}, l_i) f_{k+1|k}(\eta_1^{j_i}|x_k^{j_i}, l_i) p_S(x_k^{j_i}, l_i)}{f_{k+1|k}(\eta_0^{j_i}|x_k^{j_i}, l_i)} |\det(\dot{T}^{j_i}(\eta_0^{j_i}))| \omega_k^{j_i}, \tag{33}$$

where we employed the label-dependent transition kernel $f_{k+1|k}(\eta_0^{j_i}|x_k^{j_i}, l)$ as the prior for the flow.

A similar particle flow is achievable for the case of birth particles. At time $k+1$, consider the case of a birth target (x_i, l_i) and let $\{\eta_0^{j_i}\}_{j_i=1}^N$ be a set of particles sampled from the prior $p_B(x_i, l_i)$ and $\{\eta_1^{j_i}\}_{j_i=1}^N$ be the invertible-flow transformation of these particles. We can approximate $\hat{p}_{k+1}^{(I)}(x_i, l_i)$ with the set of weighted particles $\{(\omega_{k+1}^{j_i}, \eta_1^{j_i})\}_{j_i=1}^N$, where the normalized weights ($\sum_{j_i=1}^N \omega_{k+1}^{j_i} = 1$) are proportional to

$$\omega_{k+1}^{j_i} \propto \frac{\tilde{h}_{\bar{i}}(z_{k+1}|\eta_1^{j_i}, l_i) p_B(\eta_1^{j_i}, l_i)}{p_B(\eta_0^{j_i}, l_i)} |\det(\dot{T}^{j_i}(\eta_0^{j_i}))|. \tag{34}$$

4. SIMULATION AND RESULTS

In this section we compare the multi-target tracking performances of the TBPF-Mδ-GLMB, the UKF-SMδ-GLMB, the BPF-SMδ-GLMB and the PFPF-SMδ-GLMB filters for an acoustic localization scenario. The PFPF-SMδ-GLMB filter employs the EDH variant of the PFPF filter of.[18]

4.1 Simulation setup

We construct a multi-target tracking scenario where the number of targets is time-varying. Targets are assumed to evolve in a two dimensional Cartesian system. Target state vectors are taken to be $x_k = [p_k^x, p_k^y, \dot{p}_k^x, \dot{p}_k^y]^T$, where p_k^x and p_k^y represent the target coordinates and $\dot{p}_k^x$ and $\dot{p}_k^y$ are its velocities along the two axes. The kinematic model for the i-th target is a white noise acceleration model:

$$x_{k+1,i} = F_{k+1} x_{k,i} + v_{k+1,i}. \tag{35}$$

The state transition matrix is defined as $F_k = \left[\begin{smallmatrix} I_2 & T_S I_2 \\ 0_2 & I_2 \end{smallmatrix}\right]$ where $T_s = 1$sec is the sampling period; 0_n and I_n are the zero and identity matrices of size n. The process noise is taken to be $v_k \sim \mathcal{N}(0, Q_k)$ where for generating the tracks we employed $Q_k = \frac{1}{20}\left[\begin{smallmatrix} 1/3 I_2 & 0.5 I_2 \\ 0.5 I_2 & I_2 \end{smallmatrix}\right]$, while for tracking we employ $Q_k = \left[\begin{smallmatrix} 3 I_2 & 0.1 I_2 \\ 0.1 I_2 & 0.03 I_2 \end{smallmatrix}\right]$. The process noise covariance entries are larger for filtering than those used for generating the true tracks since we suppose the target model to be only approximately known for tracking. Additionally, the target probability of survival is taken to

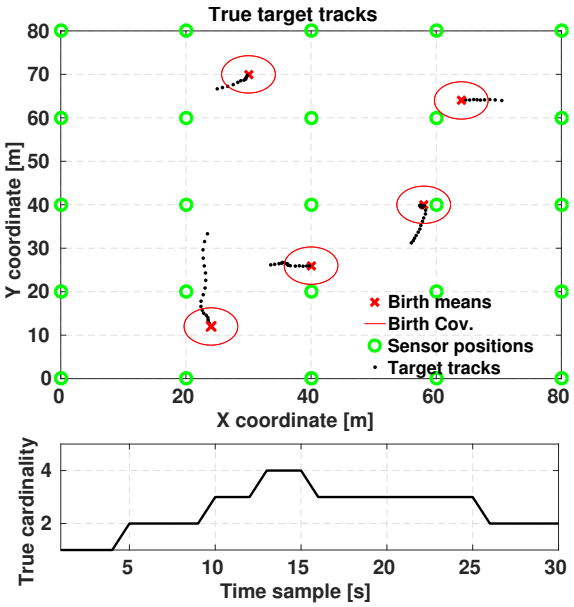

Figure 1. The true number of targets and an example of tracks. Targets are born at locations marked with ×. Sensor placements are marked with ◯.

be a constant $p_S(x,l) = 0.99$. Note that the target propagation model is not made dependent on the target label. An instance of target tracks can be observed in Fig. 1 along side the true number of targets, i.e., true cardinality of the set of targets. In the subsequent simulations, the number of targets and their birth coordinates are identical while the acceleration noise is randomly generated in each Monte Carlo trial. Additionally from Fig. 1, we can observe the layout of the 25 acoustical sensors in an uniformly spaced X-Y grid. For a sensor s placed at coordinates $(s^x,\, s^y)$, the superpositional measurement model is

$$z_{k,s} = \sum_{i=1}^{N(k)} \frac{\Psi}{\sqrt{(p_k^x - s^x)^2 + (p_k^y - s^y)^2} + d_0} + w_{k,s}, \tag{36}$$

where $\Psi = 10$ is the source signal amplitude, $d_0 = 0.1$ and $w_{k,s} \sim \mathcal{N}(0, \sigma_z^2)$ is the measurement noise that is independent for each sensor and independent from the targets. Note the superpositional nature of (36), where all $N(k)$ targets contribute to the sensor measurement.

Throughout the following section, we employ the Optimum SubPattern Assignment (OSPA) error metric[25] that incorporates both position and cardinality errors. The reported OSPA distances are evaluated between the true target tracks and the estimated tracks and hence the error is reported in meters. The two parameters of the OSPA distance are the order and the cut-off, which are set to 1 and 10m in our simulations.

4.2 Numerical results

Several simulation scenarios are created by modifying the measurement noise variance. First we investigate a set of σ_z values that ensure highly-informative measurements. The UKF-SMδ-GLMB, BPF-SMδ-GLMB (with 20k particles per target) and the PFPF-SMδ-GLMB (with 10k particles per target) are considered in this simulation scenario. For the 3 methods, the OSPA error averaged over 100 Monte Carlo runs is reported in Fig. 2. Note the improved performance of the PFPF-SMδ-GLMB filter with respect to the BPF-SMδ-GLMB filter for highly-informative measurements. In this case, the flow induced proposal helps the PFPF-SMδ-GLMB filter outperform the BPF-SMδ-GLMB filter even with fewer particles. For each Monte Carlo run, we compute the time-averaged OSPA error and we report the mean time-averaged OSPA values in Table 4.2. Additionally, in Table 4.2 we also present the average run-time per time step of the different filters. Note the relatively similar run-times of the PFPF-SMδ-GLMB filter with the BPF-SMδ-GLMB filter for the $\sigma_z \in \{0.001, 0.0005, 0.0003\}$ cases, where it also

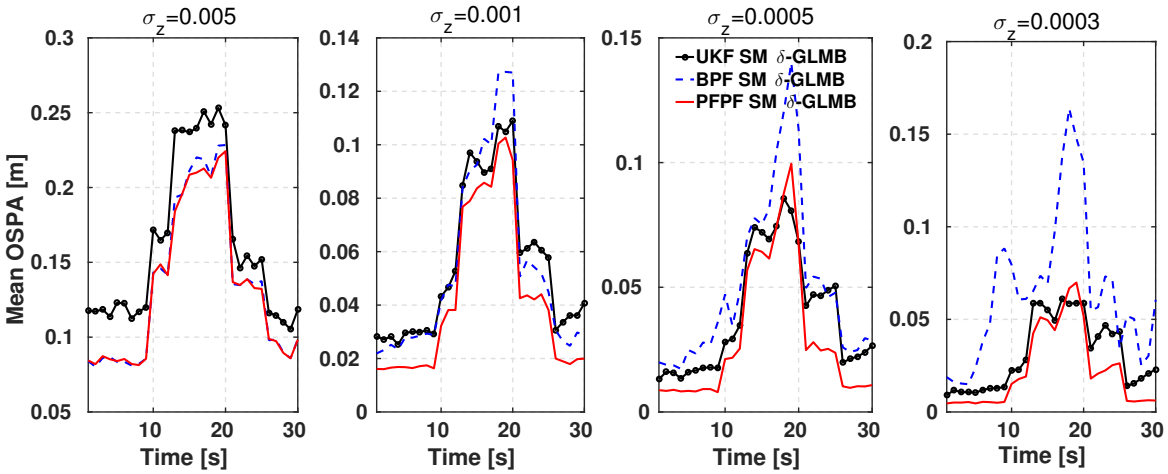

Figure 2. Average OSPA error for different values of σ_z - highly informative measurement case.

outperforms all methods in terms of OSPA error. The TBPF-Mδ-GLMB filter is not presented for these highly informative measurement cases since it greatly under-performed for any practical choice of number of particles and size of the n-tuple set Υ.

In a second simulation, we investigate the aforementioned methods together with the TBPF-Mδ-GLMB filter for a less informative measurement case. In this case we employed 2000 particles per target for BPF-SMδ-GLMB filter, 500 particles per target for the PFPF-SMδ-GLMB filter and 200 particles per target coupled with $|\Upsilon| = |\Upsilon_i| = 50 \ \forall \ i \in [1, \ n]$ for the TBPF-Mδ-GLMB filter. In Fig. 3 observe the OSPA values as a function of time and averaged over 100 Monte Carlo runs while in Table 4.2 we present the mean time-averaged OSPA values coupled with average run-times per time step. Note that in the case $\sigma_z = 0.1$ the PFPF-SMδ-GLMB filter is outperformed by the BPF-SMδ-GLMB filter both in terms of OSPA error and run-time. The higher measurement noise causes the particle flow to produce inaccurate proposals and leads to less precise track estimates which in turn result in the creation of more GLMB hypotheses and the increase in run-time. Note that for $\sigma_z = 0.1$ the TBPF-Mδ-GLMB filter has slightly higher OSPA with respect to the other methods but the run-time of the filter still remains prohibitively large. Additionally, for $\sigma_z = 0.01$ from Table 4.2 observe the significant decrease in performance of the TBPF-Mδ-GLMB filter caused by the insufficient number pf particles per target and n-tuples $|\Upsilon|$. From Fig. 3 and for the case of $\sigma_z = 0.01$, we observe a significant increase in OSPA error after time step 10 when the umber of targets increases to 3. The TBPF-Mδ-GLMB filter performance degrades when number of targets is high and the measurements are informative since the number ($|\Upsilon| = 50$) of n-tuples becomes insufficient to explore the space $\mathbb{X}^n$ and thus leads to a poor estimation of the hypothesis weight of (16). The poor and often under-estimation of hypothesis weights of the TBPF-Mδ-GLMB filter leads to the filter wrongfully dropping hypotheses that are otherwise informative, which also explains the reduced run-time of the filter for $\sigma_z = 0.01$.

	$\sigma_z = 0.005$	$\sigma_z = 0.001$	$\sigma_z = 0.0005$	$\sigma_z = 0.0003$
$\overset{UKF}{SM\delta-GLMB}$	.16m 0.055sec	.055m 0.044sec	.039m 0.040sec	.031m 0.038sec
$\overset{BPF}{SM\delta-GLMB}$	.13m 0.83sec	.054m 0.87sec	.050m 0.70sec	.064m 0.67sec
$\overset{PFPF}{SM\delta-GLMB}$	.13m 1.12sec	.042m 0.88sec	.03 0.81sec	.022m 0.80sec

Table 1. Mean time-averaged OSPA values and mean run-time per time step for highly-informative measurements.

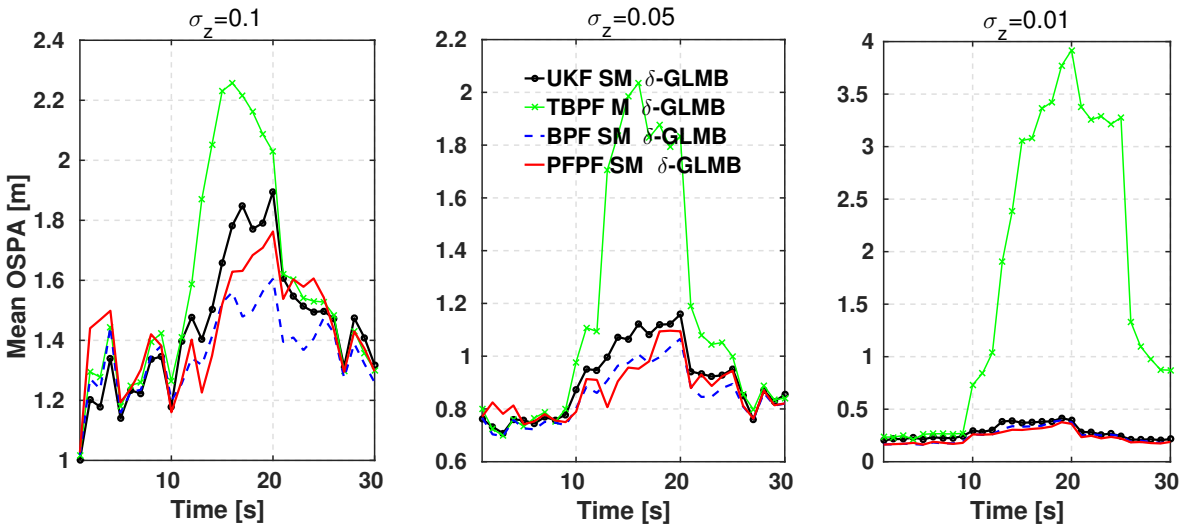

Figure 3. Average OSPA error for different values of σ_z - high variance measurement noise.

	$\sigma_z = 0.1$	$\sigma_z = 0.05$	$\sigma_z = 0.01$
$\underset{M\delta-GLMB}{TBPF}$	1.58m 17.5sec	1.15m 11.2sec	1.71m 3.5sec
$\underset{SM\delta-GLMB}{UKF}$	1.45m 0.79sec	0.9m 0.41sec	0.28m 0.06sec
$\underset{SM\delta-GLMB}{BPF}$	1.36m 1.3sec	0.85m 0.71sec	0.25m 0.13sec
$\underset{SM\delta-GLMB}{PFPF}$	1.43m 8.7sec	0.87m 4.9sec	0.23m 0.46sec

Table 2. Mean time-averaged OSPA values and mean run-time for high noise variance cases.

5. CONCLUSIONS

In this paper we proposed a superpositional marginalized δ-GLMB filter for superpositional observation models. Additionally, we provide both a bootstrap and a particle flow particle filter implementation of the proposed filter. The particle flow superpositional marginalized δ-GLMB filter is shown to provide more accurate track estimates for highly-informative measurements.

ACKNOWLEDGMENTS

This work was supported by PWGSC contract W7707-145675/001/HAL funded by Defence R&D Canada.

REFERENCES

[1] Bar-Shalom, Y., Daum, F., and Huang, J., "The probabilistic data association filter," *IEEE Control Syst. Mag.* **29**, 82–100 (December 2009).

[2] Saucan, A.-A., Chonavel, T., Sintes, C., and Le Caillec, J.-M., "3-D bathymetric reconstruction in multi-path and reverberant underwater environments," in [*Proceedings of the 21st International Conference on Image Processing (ICIP)*], (2014).

[3] Saucan, A.-A., Sintes, C., Chonavel, T., and Le Caillec, J.-M., "Model-based adaptive 3D sonar reconstruction in reverberating environments," *IEEE Trans. Image Process.* **24**, 2928–2940 (Oct. 2015).

[4] Mahler, R., "Multitarget Bayes filtering via first-order multitarget moments," *IEEE Trans. Aerosp. Electron. Syst* **39**, 1152 – 1178 (Oct. 2003).

[5] Georgescu, R. and Willett, P., "The GM-CPHD tracker applied to real and realistic multistatic sonar data sets," *IEEE J. Ocean. Eng.* **37**, 220–235 (April 2012).

[6] Georgescu, R. and Willett, P., "The multiple model CPHD tracker," *IEEE Trans. Signal Process.* **60**, 1741–1751 (April 2012).

[7] Maggio, E. and Cavallaro, A., "Learning scene context for multiple object tracking," *IEEE Trans. Image Process.* **18**, 1873–1884 (Aug. 2009).

[8] Mullane, J., Vo, B.-N., Adams, M. D., and Vo, B.-T., "A random-finite-set approach to Bayesian SLAM," *IEEE Trans. Robot.* **27**, 268–282 (April 2011).

[9] Vo, B.-T. and Vo, B.-N., "Labeled random finite sets and multi-object conjugate priors," *IEEE Trans. Signal Process.* **61**, 3460–3475 (Jul. 2013).

[10] Vo, B.-N., Vo, B.-T., and Phung, D., "Labeled random finite sets and the Bayes multi-target tracking filter," *IEEE Trans. Signal Process.* **62**, 6554–6567 (Dec. 2014).

[11] Vo, B.-N., Vo, B.-T., and Hoang, H. G., "An efficient implementation of the Generalized Labeled multi-Bernoulli filter," *IEEE Trans. Signal Process.* **65**, 1975–1987 (April 2017).

[12] Vo, B.-N., Vo, B.-T., Pham, N.-T., and Suter, D., "Joint detection and estimation of multiple objects from image observations," *IEEE Trans. Signal Process.* **58**, 5129–5141 (Oct. 2010).

[13] Nannuru, S., Coates, M., and Mahler, R., "Computationally-tractable approximate PHD and CPHD filters for superpositional sensors," *IEEE J. Sel. Topics Signal Process.* **7**, 410 – 420 (Jun. 2013).

[14] Saucan, A.-A., Chonavel, T., Sintes, C., and Caillec, J. M. L., "CPHD-DOA tracking of multiple extended sonar targets in impulsive environments," *IEEE Trans. Signal Process.* **64**, 1147–1160 (Mar. 2016).

[15] Papi, F. and Kim, D. Y., "A particle multi-target tracker for superpositional measurements using labeled random finite sets," *IEEE Trans. Signal Process.* **63**, 4348–4358 (Aug 2015).

[16] Papi, F., Vo, B.-N., Vo, B.-T., Fantacci, C., and Beard, M., "Generalized labeled multi-Bernoulli approximation of multi-object densities," *IEEE Trans. Signal Process.* **63**, 5487–5497 (Oct. 2015).

[17] Gordon, N., Salmond, D., and Smith, A., "Novel approach to nonlinear/non-Gaussian Bayesian state estimation," *IEE Proc. F - Radar, Signal Process.* **140**, 107–113 (Apr. 1993).

[18] Li, Y. and Coates, M., "Particle filtering with invertible particle flow," `arXiv:1607.08799 [stat.ME]`.

[19] Mahler, R., [*Statistical Multisource-Multitarget Information Fusion*], Artech House, Norwood, MA (2007).

[20] Julier, S. J. and Uhlmann, J. K., "Unscented filtering and nonlinear estimation," *Proc. IEEE* **92**, 401–422 (Mar. 2004).

[21] Julier, S. J. and Uhlmann, J. K., "Corrections to "Unscented Filtering and Nonlinear Estimation"," *Proc. IEEE* **92**, 1958 (Dec. 2004).

[22] Saucan, A.-A., Li, Y., and Coates, M., "Particle flow SMC δ-GLMB filter," in [*Proc. IEEE Int. Conf. Acoust. Speech Signal Process. (ICASSP)*], (March 2017).

[23] Daum, F., Huang, J., and Noushin, A., "Exact particle flow for nonlinear filters," in [*Proc. SPIE Conf. Signal Process., Sensor Fusion, Target Recog.*], 769704 (Apr. 2010).

[24] Ding, T. and Coates, M. J., "Implementation of the Daum-Huang exact-flow particle filter," in [*Proc. IEEE Statistical Signal Process. Workshop (SSP)*], 257–260 (Aug. 2012).

[25] Schuhmacher, D., Vo, B.-T., and Vo, B.-N., "A consistent metric for performance evaluation of multi-object filters," *IEEE Trans. Signal Process.* **56**, 3447–3457 (Aug. 2008).